

Hydrological Sciences Journal

Publication details, including instructions for authors and subscription information:
<http://www.tandfonline.com/loi/thsj20>

Global projections of changing risks of floods and droughts in a changing climate

YUKIKO HIRABAYASHI ^a, SHINJIRO KANAE ^b, SEITA EMORI ^c, TAIKAN OKI ^b & MASAHIKE KIMOTO ^d

^a Interdisciplinary Graduate School of Medicine and Engineering, University of Yamanashi, 4-3-11 Takeda, Kofu, Yamanashi, 400-8511, Japan E-mail:

^b Institute of Industrial Science, The University of Tokyo, 4-6-1, Komaba, Meguro-ku, Tokyo, 153-8505, Japan

^c Atmospheric Environment Division, National Institute for Environmental Studies, 16-2 Onogawa, Tsukuba, Ibaraki, 305-0053, Japan

^d Center for Climate System Research, The University of Tokyo, 5-1-5, Kashiwanoha, Kashiwa-shi, Chiba, 277-8568, Japan

Version of record first published: 18 Jan 2010

To cite this article: YUKIKO HIRABAYASHI, SHINJIRO KANAE, SEITA EMORI, TAIKAN OKI & MASAHIKE KIMOTO (2008): Global projections of changing risks of floods and droughts in a changing climate, *Hydrological Sciences Journal*, 53:4, 754-772

To link to this article: <http://dx.doi.org/10.1623/hysj.53.4.754>

PLEASE SCROLL DOWN FOR ARTICLE

Full terms and conditions of use: <http://www.tandfonline.com/page/terms-and-conditions>

This article may be used for research, teaching, and private study purposes. Any substantial or systematic reproduction, redistribution, reselling, loan, sub-licensing, systematic supply, or distribution in any form to anyone is expressly forbidden.

The publisher does not give any warranty express or implied or make any representation that the contents will be complete or accurate or up to date. The accuracy of any instructions, formulae, and drug doses should be independently verified with primary sources. The publisher shall not be liable for any loss, actions, claims, proceedings, demand, or costs or damages whatsoever or howsoever caused arising directly or indirectly in connection with or arising out of the use of this material.

Global projections of changing risks of floods and droughts in a changing climate

**YUKIKO HIRABAYASHI¹, SHINJIRO KANAE², SEITA EMORI³,
TAIKAN OKI² & MASAHIKE KIMOTO⁴**

¹ *Interdisciplinary Graduate School of Medicine and Engineering, University of Yamanashi, 4-3-11 Takeda, Kofu, Yamanashi 400-8511, Japan*
hyukiko@yamanashi.ac.jp

² *Institute of Industrial Science, The University of Tokyo, 4-6-1, Komaba, Meguro-ku, Tokyo 153-8505, Japan*

³ *Atmospheric Environment Division, National Institute for Environmental Studies, 16-2 Onogawa, Tsukuba, Ibaraki 305-0053, Japan*

⁴ *Center for Climate System Research, The University of Tokyo, 5-1-5, Kashiwanoha, Kashiwa-shi, Chiba 277-8568, Japan*

Abstract Simulated daily discharge derived from a relatively high-resolution (approximately 1.1-degree) general circulation model was used to investigate future projections of extremes in river discharge under global warming. The frequency of floods was projected to increase over many regions, except those including North America and central to western Eurasia. The drought frequency was projected to increase globally, while regions such as northern high latitudes, eastern Australia, and eastern Eurasia showed a decrease or no significant changes. Changes in flood and drought are not explained simply by changes in annual precipitation, heavy precipitation, or differences between precipitation and evapotranspiration. Several regions were projected to have increases in both flood frequency and drought frequency. Such regions show a decrease in the number of precipitation days, but an increase in days with heavy rain. Several regions show shifts in the flood season from springtime snowmelt to the summer period of heavy precipitation.

Key words drought; flood; global warming; river discharge

Projections globales des changements dans les risques de crues et de sécheresses liés au changement climatique

Résumé Les débits journaliers simulés à partir d'un modèle de circulation générale d'une résolution relativement haute (approximativement 1.1 degré) ont été utilisés pour étudier les projections futures des extrêmes des débits de rivières dans le contexte du réchauffement global. Une augmentation de la fréquence des crues est projetée pour de nombreuses régions, à l'exception des régions incluant l'Amérique du Nord et l'Eurasie centrale à occidentale. L'augmentation de la fréquence des sécheresses est projetée globalement, alors que les régions des hautes latitudes boréales, de l'Australie orientale et de l'Eurasie orientale présentent une décroissance ou une absence de changement significatif. Les changements pour les crues et les sécheresses ne s'expliquent pas simplement par des changements dans les précipitations annuelles, les fortes précipitations ou les différences entre précipitation et évapotranspiration. Les projections de plusieurs régions présentent des augmentations à la fois dans la fréquence des crues et dans celle des sécheresses. De telles régions présentent une décroissance dans le nombre de jours de précipitation, mais une augmentation des jours de forte précipitation. Plusieurs régions présentent des décalages de la saison des crues, de la période printanière de fonte nivale vers la période estivale de fortes précipitations.

Mots clefs sécheresse; crue; réchauffement global; débit de rivière

1 INTRODUCTION

Several recent studies have reported trends over the past several decades in the frequency of heavy to extreme hydrological events. A common and popular topic for such analyses has been extreme precipitation events (e.g. Kunkel *et al.*, 2003; Kanae *et al.*, 2004), because long-term continuous gauge observations are available for several decades for many stations around the globe. Future extreme daily precipitation projections have also been estimated and discussed based on various climate change simulations (e.g. Emori *et al.*, 2005). However, there have been insufficient studies of future projections of extremes in global river discharge in climate change simulations. This is primarily because of the limitation of spatial resolution in general circulation models (GCMs).

Milly *et al.* (2002) investigated changes in flood extremes using monthly river discharge data for both gauge observations and GCM simulations. They found that the risk of great floods increased during the 20th century, mainly over the northern high latitudes, and that this increase

may continue. Limitations in the spatial resolution of their GCM allowed the analysis of monthly averaged discharge over 29 river basins larger than 200 000 km² in area, where the coarse spatial resolution of the GCM can resolve the basin and where the annual maximum monthly mean flows are correlated with annual maximum instantaneous flows.

Dai *et al.* (2004) used temperature and gauge-based precipitation data to estimate the Palmer drought severity index (Palmer, 1965) for the USA. The method of Dai *et al.* (2004) is simple and has great potential for projecting future drought, viewed mainly as a shortage of precipitation. However, low river flows (streamflow droughts) must also be considered, because many regions are irrigated with river water. Andreadis *et al.* (2005) used a land surface model (LSM) driven by historical atmospheric data on a 1/2° grid to estimate water budget in the 20th century over the USA and found that the shortage of storages in soil moisture and in runoff were not always coincident in space and time. This study implies that low river flows may not be estimated simply from vertical water and energy balances, such as soil moisture or precipitation minus evapotranspiration. This indicates the importance of global estimation of low river flows.

To date, computer technology has allowed long-term global estimates of hydrological components using a GCM containing ocean, atmosphere and land surface sub-modules (hereafter referred to as "coupled ocean–atmosphere–land" GCM) with relatively high spatial resolution (T106, approximately 1.1 degree) for historical and future climate change scenario forcing. The estimated river discharge from the high-resolution GCM named the Model for Interdisciplinary Research on Climate (MIROC) can be used to predict future local hydrological extremes for risk assessments. Kimoto *et al.* (2005) showed that long-term global climate simulated by the MIROC implemented herein shows a more realistic geographical distribution and more reasonable numbers of days with precipitation than do simulations with coarser resolutions using the same model. This suggests that our projection of future extremes provides state-of-the-art results based on the high-resolution GCM. Because extremes in river discharge are strongly affected by the spatial distribution of the precipitation intensity within a basin, an atmospheric sub-module in a high-resolution GCM may be indispensable for the accurate estimation of extremes in river discharge.

The aim of this study was to demonstrate future projections of extremes in global river discharge, i.e. flood and drought, estimated using the daily modelled discharge by the MIROC. The global warming simulation with relatively high spatial resolution of the MIROC will provide a detailed picture of future extremes in river discharge, even over small basins that have not been distinguished by Milly *et al.* (2002). It is essential to show projections of changes in extreme discharge under global warming using daily discharge data, since previous studies discussed future projections on water-related disasters mainly in terms of changes in monthly means of precipitation or in discharge. At present, the MIROC is the only GCM used in the global warming experiment with relatively high resolution. Therefore, we focus on the results of a single GCM projection, while future studies with other high-resolution GCMs are expected.

The global validation of flood characteristics in the GCM is attempted using available gauge observations and a long-term off-line simulation. Because the method for estimating drought uses a relative threshold value of discharge, the characteristics of droughts in the 20th century simulation in the GCM cannot be validated directly. The definitions of flood and drought are based upon severe flood and drought disasters recorded in a disaster database, so that statistically defined "extremes" in the time series of daily river discharge replicate historical disastrous floods and droughts. Finally, the relationship of future changes in atmospheric forcing to changes in flood and drought over large river basins is discussed. The discussion and the methodology used to validate extremes in the GCM discharge here can be applied to other GCMs.

2 DATA

Three long-term daily river discharge data sets are described below: future projections of flood and drought from daily discharge estimated by the MIROC; daily gauge observations; and daily discharge estimation by off-line simulation are used to validate the extreme discharge estimated by the MIROC.

2.1 GCM output (1901–2100) by the MIROC

The GCM output analysed was obtained from a climate change simulation using the MIROC. The MIROC is a coupled ocean-atmosphere-land GCM developed collaboratively by the Center for Climate System Research (CCSR) at the University of Tokyo, the National Institute for Environmental Studies (NIES, Japan), and the Frontier Research Center for Global Change (FRCGC) at the Japan Agency for Marine-Earth Science and Technology. A complete description of the model is provided by K-1 model developers (2004). Aerosol distribution is prescribed in the MIROC, not calculated interactively, and the second indirect effect of aerosols is suppressed. The MIROC has T106 spectral truncation in the horizontal plane (320×160 grid for the globe) and 56 atmospheric layers. The ocean resolution is $1/4^\circ \times 1/6^\circ$ with 48 levels. Sub-modules for land, sea ice, and five soil layers also use the T106 grid. The MIROC includes the Minimal Advanced Treatments of Surface Interaction and Runoff (MATSIRO) LSM (Takata *et al.*, 2003). The MATSIRO model incorporates spatially-distributed soil properties and vegetation coverage, and computes vertical fluxes of energy and water for each grid cell. Vegetation processes in MATSIRO are derived mainly from the Simple Biosphere 2 (SiB2) model (Sellers *et al.*, 1996); these include the multilayer canopy model by Watanabe (1994), and runoff generation processes as suggested by Famiglietti & Wood (1991) and Stieglitz *et al.* (1997), that are based on the original topography-based TOPMODEL (Beven & Kirkby, 1979).

Milly *et al.* (2005) showed that annual runoff estimated by the MIROC matches observations well. Runoff at each T106 spectral grid of MIROC was assigned to a 1° grid using the nearest-neighbour method; these were then integrated for the river basin using the total runoff integrating pathways (TRIP) model (Oki & Sud, 1998) with a constant discharge velocity of 0.5 m/s. The MIROC simulation periods included the retrospective simulations of the 20th century for 1901–2000 and the SRES A1B (IPCC, 2000) future scenario for 2001–2100. The SRES A1B assumes a future world of very rapid economic growth and a mix of technological developments and fossil fuel use. Emori *et al.* (2005) and Kimoto *et al.* (2005) have discussed the future projection of precipitation by this simulation. The global warming experiment of the MIROC showed the highest temperature transient among the Intergovernmental Panel on Climate Change (IPCC) Fourth Assessment Report (AR4) climate models due to its large ice-albedo feedback and lower ocean heat uptake. Because the MIROC shows better agreement with the observed factors on ice-albedo feedback and ocean heat uptake than the GCM with lower horizontal resolution, the future projection of temperature in the MIROC is not considered to be unrealistic (Yokohata *et al.*, 2007). Since higher temperature rise normally leads to higher acceleration of the water cycle, the projected changes in extremes in the water cycle in the MIROC are expected to be higher than those of other GCMs.

Figure 1 shows future changes with respect to 20th century values of annual precipitation, annual evapotranspiration, the intensity of the annual fourth largest daily precipitation event (approximately 99th percentile), and the annual mean surface temperature. The MIROC yielded increased annual precipitation under the future scenario over most northern high latitudes, eastern Asia, and central to eastern Africa. The region of increased evapotranspiration nearly overlaps the region of increased annual precipitation. Heavy precipitation increases globally, except for the regions including the western coasts of the USA, parts of Chile and the Arabian Peninsula. Surface temperature increases globally in the 21st century, most notably over the northern high latitudes.

2.2 Gauge observations compiled by the GRDC

Gauge-based daily discharge observations collected by the Global Runoff Data Center (GRDC) were used to validate discharge extremes estimated by the MIROC. The analysis used daily discharge observations at 724 stations of the GRDC that spanned at least 30 of the 60 years from 1941 to 2000, for areas $>100\,000\text{ km}^2$. When estimating drought indices from the data, Student's *t* test to detect the artificial control of river discharge, e.g. reservoir operation, was applied to the annual mean discharge.

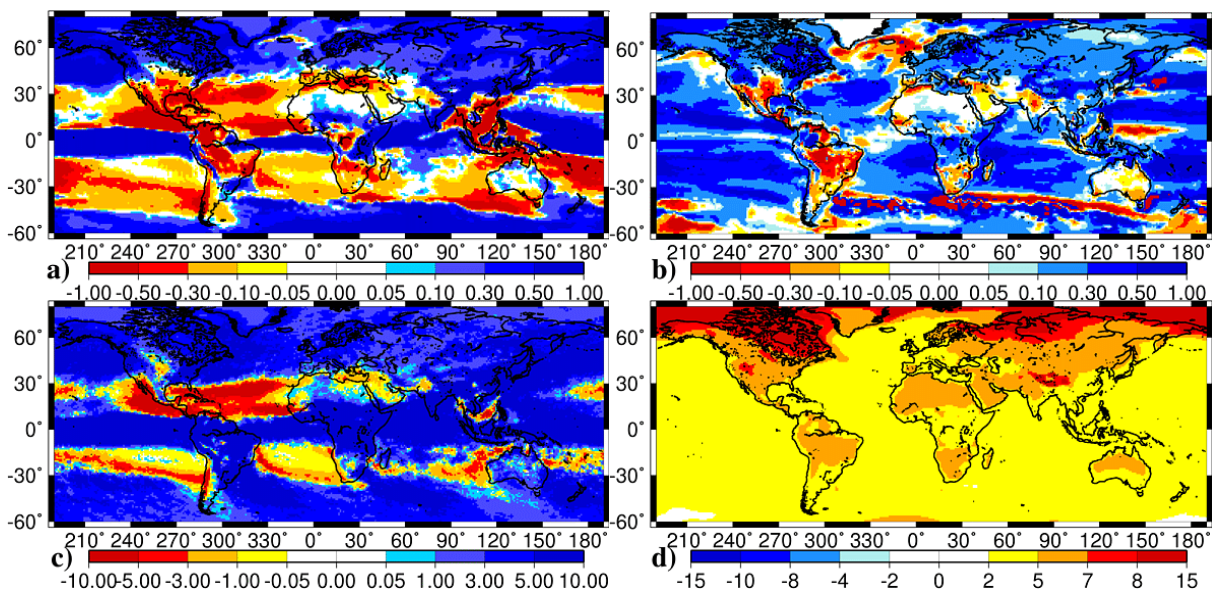


Fig. 1 Future (2071–2100) changes from present-day (1901–2000) values of: (a) annual precipitation, (b) annual evapotranspiration, (c) intensity of annual fourth largest daily precipitation, and (d) annual mean surface temperature.

2.3 Off-line hydrological estimation by MATSIRO LSM (1901–2000)

A global off-line simulation for 1901–2000 using the MATSIRO LSM, which is incorporated into the MIROC model as a land surface sub-module, was used to validate the 20th century simulation by the MIROC at regions lacking long-term discharge observations with which to estimate extremes.

Hirabayashi *et al.* (2005) described the design of the off-line simulation in detail. The MATSIRO model was driven by atmospheric forcing obtained from available observations and several statistical and empirical methods, because there were not sufficient atmospheric data to drive the model for relatively longer periods. The monthly observations of precipitation, number of rainy days, and maximum and minimum temperature provided by the Climate Research Unit (CRU; Mitchell & Jones, 2005) were used to derive diurnal to sub-diurnal atmospheric forcing using a statistical weather generator and several empirical equations suggested by Nijssen *et al.* (2000). Several parameters required in the methods to obtain the sub-daily atmospheric forcing data were derived from available global daily data sets for the last several decades of the 20th century, which were assumed to be constant, and applied over the entire 20th century. Runoff at each grid was integrated using the TRIP model. The estimation by the off-line simulation showed good correlations for long-term observed variation in river discharge, snow area and soil moisture. A GCM simulation using soil moisture and snow estimated from the off-line simulation as a boundary, showed an increase in the predictability of boreal summer precipitation (Kanae *et al.*, 2006), which indirectly indicates that the long-term hydrological components estimated in the off-line simulation are reasonable. The ability of the off-line simulation to estimate extremes in discharge is validated in the next section.

To eliminate discharge estimation driven by atmospheric forcing based on poorly gauged precipitation observations, the discharge data at poorly gauged grid locations in the off-line simulation were screened out by the density of gauge observations for precipitation of upper basins of the grid cells. This study used 30 gauges per 10^6 km^2 , as suggested by Oki *et al.* (1999), as the critical density for the screening procedure. This screening of poorly gauged grid locations resulted in fewer plots in the off-line simulation than available gauge observations, especially for stations at low latitudes.

3 FLOOD

To describe flood events, we analysed 100-year floods, defined as river discharge that has a probability of being exceeded in any given year of 0.01. The time series of annual maximum daily discharge was fitted using the moment fitting method for a Gumbel distribution (Gumbel, 1960) at each grid. The fitting method uses two moment parameters, a and b . The probability distribution function (PDF) of annual maximum daily discharge x is defined as:

$$\begin{aligned} f_x(x) &= a \cdot e^{-a(x-b)-e^{-a(x-b)}} \\ \mu_x &= b + \frac{\nu}{a} \\ \sigma_x &= \frac{\pi}{\sqrt{6a}} \end{aligned} \quad (1)$$

where $f_x(x)$ is the PDF of x , ν is Euler's constant ($= 0.57721$), and μ_x is the average and σ_x the standard deviation of x . The moment parameters (a and b) were estimated from the average and standard deviation of x in each grid as shown in equation (1).

3.1 Flood validation

The MIROC was validated using gauge data for locations where long-term gauge observations were available. The off-line simulation was also used to validate the MIROC for regions where gauge observations were not available. First, a statistical test was used to check whether the annual maximum daily discharge in the MIROC was well approximated by the Gumbel distribution. The Gumbel distribution hypothesis using the moment fitting method for the annual maximum daily discharge in MIROC was examined using the probability plot correlation coefficient (PPCC; Vogel, 1986). When the PPCC is close to 1.0, the Gumbel distribution hypothesis explains the distribution of the maximum daily discharge estimated by MIROC. Vogel (1986) indicated that the critical point of the PPCC at the 90–95% significance level is approx. 0.98 when the size of the test sample is 100, and approx. 0.96 when the size of the test sample is 30. Figure 2 shows the PPCCs estimated from the annual maximum daily discharge by MIROC for 100 years from 1901 to 2000 and for 30 sample years from 1971 to 2000 at each grid. In both cases, the PPCCs were low in dry regions such as northern Africa, the Arabian Peninsula and Australia. However, for these dry regions, disasters due to high extreme discharge may be less important than other disasters such as drought. The PPCCs for 1971–2000 (Fig. 2(b)) were lower than those for 1901–2000 (Fig. 2(a)), mainly because of the shorter sample time. The averaged PPCCs over the 50 largest river basins globally for the two samples showed that 32 basins exceeded the significance level (0.98) for the 100-year sample and 43 basins exceeded the significance level (0.96) for the 30-year sample. These results indicate that the Gumbel distribution hypothesis using the moment method can be applied to these large river basins. The PPCC was used to screen out regions for which the Gumbel distribution hypothesis could not be applied by MIROC to project flood.

In a second step, the distributions of the return periods estimated by the method in the off-line simulation were compared to those in the observations. In order to investigate whether the statistically estimated extremes in discharge represent actual disastrous flood, the return periods of the annual maximum daily discharge when severe flood disasters occur are examined. The disastrous flood information was extracted from the statistical disaster archives for large flooding events of the Dartmouth Flood Observatory (Brakenridge *et al.*, 2003) and the Emergency Disasters Data Base (EM-DAT) of the Office of US Foreign Disaster Assistance / Centre for Research on Epidemiology of Disasters International Disaster Database (available online at <http://www.em-dat.net>). Because these disaster databases registered floods where a certain level of damage to goods and human lives were reported, the floods that are obtained statistically from the daily discharge data sets are sometimes not included in the databases, especially over times and regions where the population is low, or for regions where damage due to disasters is not well

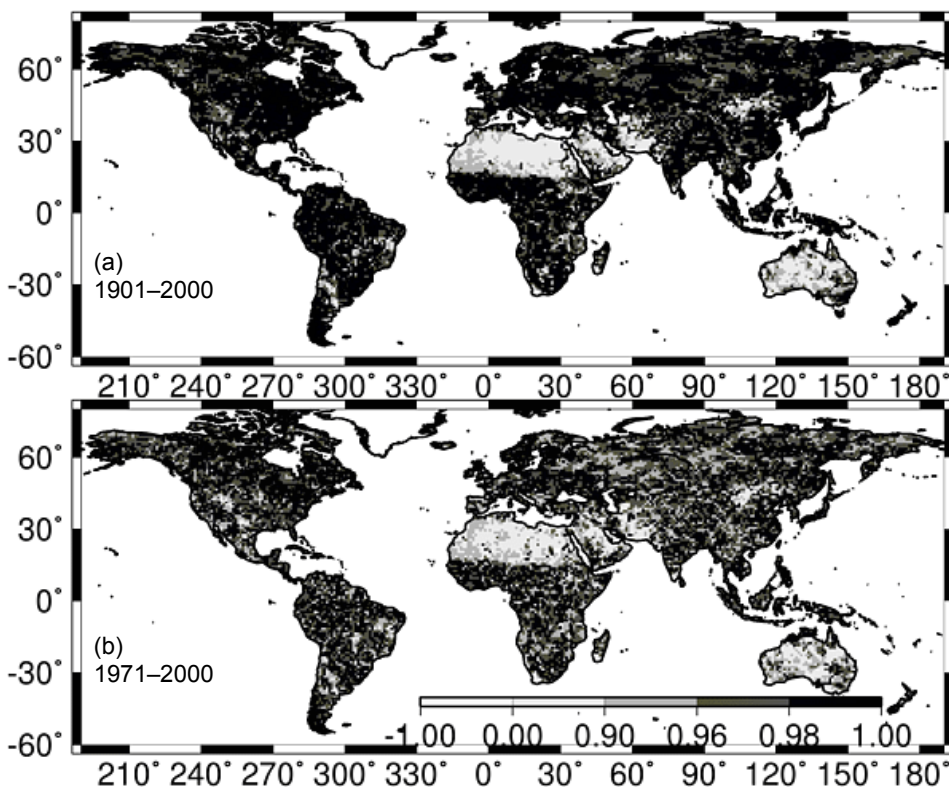


Fig. 2 Probability plot correlation coefficient (PPCC; 0-1, dimensionless) for Gumbel distribution hypothesis on the annual maximum daily discharge by MIROC for sample years: (a) 1901–2000 and (b) 1971–2000.

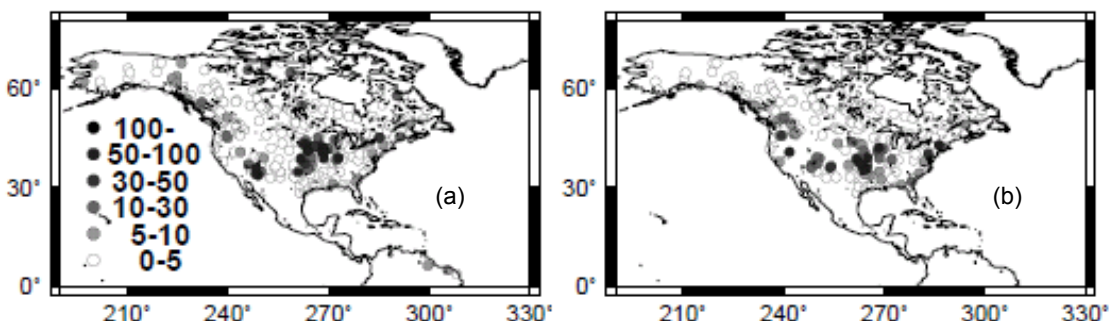


Fig. 3 Return period (year) of the annual maximum daily discharge over the USA in 1993 estimated from: (a) gauge observation and (b) off-line simulation.

summarized and reported. Nevertheless, most severe floods registered in the database can be detected from the daily discharge data. In Fig. 3, the estimated return periods of the annual maximum daily discharge are compared with those from available gauge stations over the USA in 1993, when severe flooding occurred along the Mississippi River. The dots represent stations with relatively long-term gauge observations, in which the Gumbel approximation to estimate the return period of 100-year floods could be applied. The parameters of the Gumbel distribution were estimated from all available observation periods and the return period of the annual maximum daily discharge in 1993 was estimated using these parameters. The Gumbel parameters were estimated separately for observations and the off-line simulation by using the same maximum available periods for the two data sets. Both the observations and off-line simulation showed severe floods with a long return period (30-years or longer) in the middle to upper Mississippi

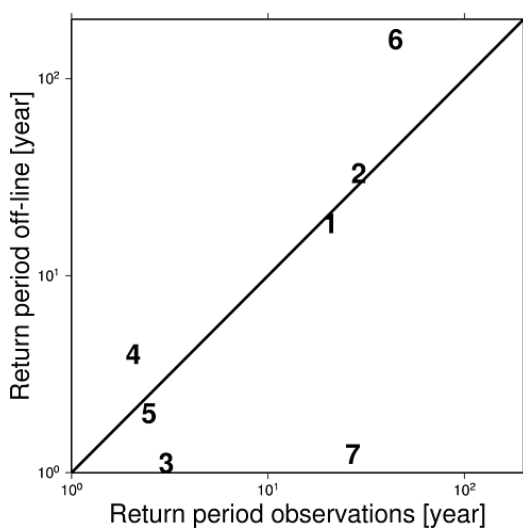


Fig. 4 Return period (year) of the annual maximum daily discharge of seven flood disasters summarized in Table 1.

Table 1 Return periods (year) of observed discharge (GRDC) and off-line simulation on severe flood disasters.

	Year	River (GRDC station)	Return period GRDC	Return period off-line
1	1940	Donau (6742500)	21.79	18.40
2	1940	Elbe (6340150)	28.90	33.07
3	1975	Donau (6742500)	3.03	1.12
4	1977	Brahmaputra (2151100)	2.06	3.99
5	1983	St Lawrence (4243150)	2.48	2.00
6	1993	Mississippi (4125801)	46.66	158.50
7	1993	Rhein (6435060)	27.00	1.24

River basin. Because the Dartmouth and EM-DAT database also show that the Mississippi flood in 1993 occurred mainly over the middle to upper basin area, it is evident that the off-line simulation reproduced the occurrence and location of such a historical flood well. In Fig. 4 the off-line simulation and observation of return periods are compared for seven selected flood disasters (Fig. 4, Table 1). All of the stations had more than 30 years of data, with PPCC > 0.9. If there were more than two stations along a flooded river, the station with the largest upper basin area was selected. Because the return period estimated by the Gumbel distribution changes exponentially, the values were plotted on a logarithmic scale. The return periods in the off-line simulation correspond to the observations, except for the case of the Rhein River flood. One of the main reasons for this is that the annual variation in the maximum daily discharge in the off-line simulation for the Rhein River was poorly correlated with the observations. An artificial control by reservoir operations, which was not implemented in the off-line simulation, may be responsible for this poor correlation. Discharge in the off-line simulation shows lower correlation with observations over cold regions (Hirabayashi *et al.*, 2005), and it may also cause the poor correlation for the Rhein River. The reason for this may be inadequate distinction of solid precipitation, low quality of precipitation forcing data due to low gauge density in mountainous regions, or the process of river freezing which is not included in the model. The overestimation of the return period in the off-line simulation at stations 3, 4 and 6 is reasonable, because our model does not include a process of decrease in discharge when floodwaters overflow the river channel and inundate a basin area, such as frequently occurs in severe flood disasters.

The land-surface sub-module in the MIROC, i.e. the off-line simulation, captures the past disastrous flood events well. However, it is difficult to compare the simulated floods in the

MIROC with historical floods, because the MIROC is a coupled ocean–atmosphere–land model and its climate may be statistically similar to observed data, but not necessarily the same as those observed each day as estimated from a weather prediction model. If significant changes in floods have already appeared in recent decades compared to the past several decades of observation, it is easy to simply check whether the same trends can be reproduced in the MIROC. For example, Zhang *et al.* (2007) investigated the results of 14 GCMs and showed that the detection and attribution of human influence on the observed changes in zonal mean of annual mean terrestrial precipitation during the 20th century is robust. However, the number of available discharge observations required to investigate such significant changes in floods is limited. If the stations that spanned at least 60 of the 80 years from 1901 to 1980 and at least 15 of the 20 years from 1981 to 2000, are assumed to be sufficiently long to investigate a trend in annual maximum daily discharge between 1901–1980 and 1981–2000, 48 stations are available from the 724 available gauges. However, statistical jumps due to artificial controls are detected by the Student's *t* test in all but four of these stations. The result of the statistical test is reasonable, because most of the stations providing observations longer than several decades are commonly located near large dams. The trend analysis for the four stations using the Monte Carlo approach (explained in detail in the next sub-section) showed that three stations show the same results for observation and MIROC; significant trends are seen for two stations and negative trend is detected for one station. For one station, the data in the MIROC show positive trend but no significant trend is seen in the observations. This inconsistency may be because the total area of the upper basin of this station is as small as the area size of one grid of the atmospheric sub-model, which leads to relatively high model sensitivity of discharge to changes in precipitation.

3.2 Projecting future flood events

The projection of flood events by the MIROC under the A1B global warming scenario is described here. The return period was estimated of floods with future discharge equivalent to that of a 100-year return period in the 20th century (1901–2000) simulation. Before estimating the change in the return period, the statistical significance of changes in the annual maximum daily discharge under the global warming simulation was tested using a Monte Carlo approach:

- (a) 1000 simulations, each performed using 30 random samples of the annual maximum daily discharge from the 20th century simulation, were averaged, and the 1000 average values were sorted in descending order; and
- (b) the annual maximum daily discharges in the projected future climate for each of 2001–2030 and 2071–2100 were averaged.

When the value of (b) is larger than the 50th sample of (a), the annual maximum daily discharge is increased in the future climate with 95% significance. The annual maximum daily discharge is decreased with 95% significance when the value of (b) is smaller than the 950th sample of (a). Figure 5 shows the comparison of statistical significance of changes in the annual maximum daily discharge between the first and last 30-year periods of the 21st century (i.e. 2001–2030 and 2071–2100) estimated by the MIROC under the SRES A1B scenario with that of the 20th century (1901–2000). In 2001–2030, only a few regions showed widespread significant changes in the annual maximum daily discharge (Fig. 5(a)), whereas in 2071–2100, most regions showed significant changes (Fig. 5(b)). The increase over regions at low latitudes, such as central Africa and India, is prominent in 2071–2100. The annual maximum daily discharge also increased significantly over central to northern South America and Australia. In contrast, the annual maximum daily discharge decreased over northern North America, western Eurasia except in the Iberian Peninsula, and northern and southern Africa, as well as parts of South America.

The return period of 100-year floods with respect to the 20th century (1901–2000) simulation (hereafter referred to as “20C 100-year flood”) changed under the future climate as predicted by the MIROC (Fig. 6). Regions with low PPCC (i.e. <0.9 during 1971–2000) were screened out. Regions that had no significant change in the annual maximum daily discharge (Fig. 5) were also

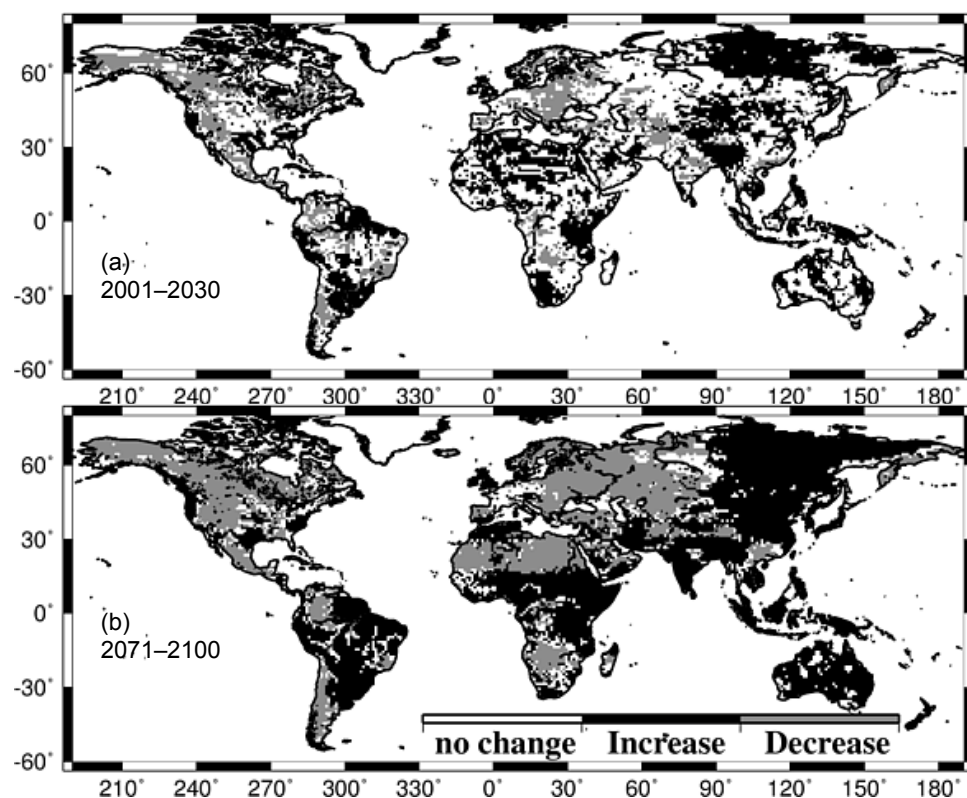


Fig. 5 Statistical significance of changes in the annual maximum daily discharge of: (a) the first and (b) the last 30 years of the 21st century, by the MIROC against those in the 20th century (1901–2000).

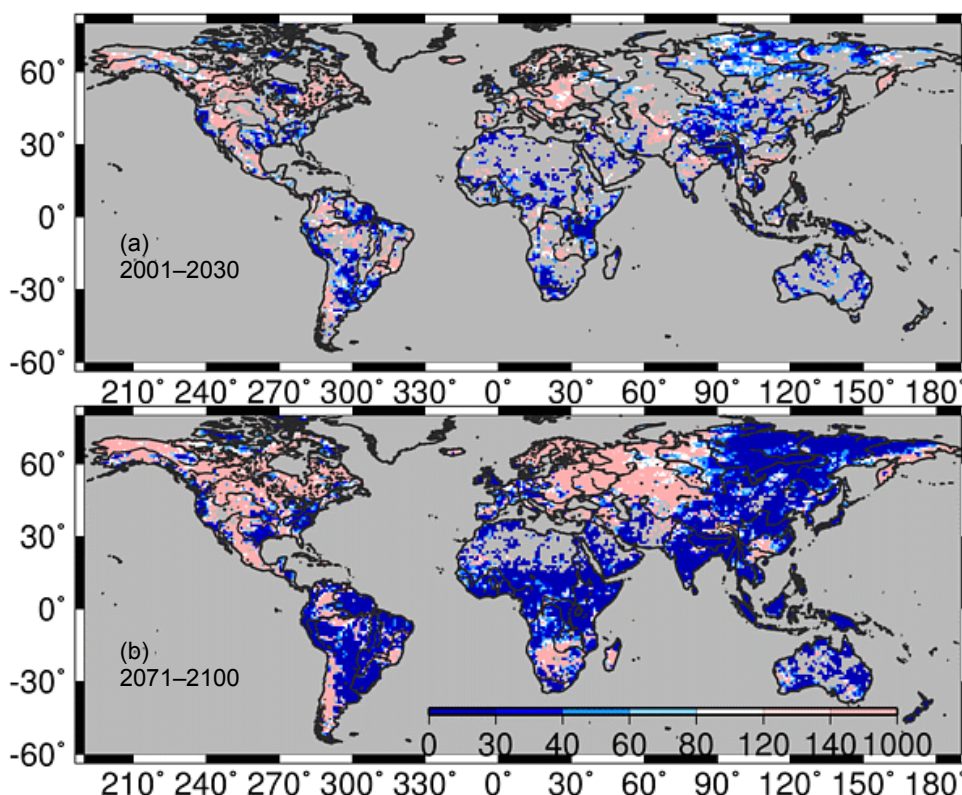


Fig. 6 Projected return period (year) of the 20C 100-year floods in the present-day (1901–2000) simulation during: (a) 2001–2030 and (b) 2071–2100 estimated by the MIROC.

screened out. A return period of less than 30 years, corresponding to that for a 20C 100-year flood in the retrospective climate, was projected in many low-latitude regions and in eastern Eurasia. In contrast, the frequencies of the extreme discharge exceeding the amount of the 20C 100-year flood decreased over central and northern North America, eastern Europe and western Russia, even though the annual precipitation and fourth largest precipitation event per year both increased in these areas (e.g. see Fig. 1).

Figure 7 shows the month of annual maximum daily discharge in the 20th century simulation (1901–2000), in the future scenario simulation (2071–2100), and the difference between them. Northern high latitudes showed a 1-month shift in the maximum discharge at most grid points. Maximum discharges in these regions occurred in spring or early summer, and their shift occurred earlier, possibly as a result of earlier snowmelt under the warmer future climate. This earlier peak at northern high latitudes causes a lower peak discharge and lower frequencies of 20C 100-year flood. Shifts in the peak by 1 month or more were evident in regions such as Eastern Europe, central and northeastern Northern America, and northern China to Mongolia. In the retrospective climate, these three regions have peak discharges during late winter to spring (February–April); the future shift moves these peak discharges by 3 or 4 months to July and August. Such a shift in

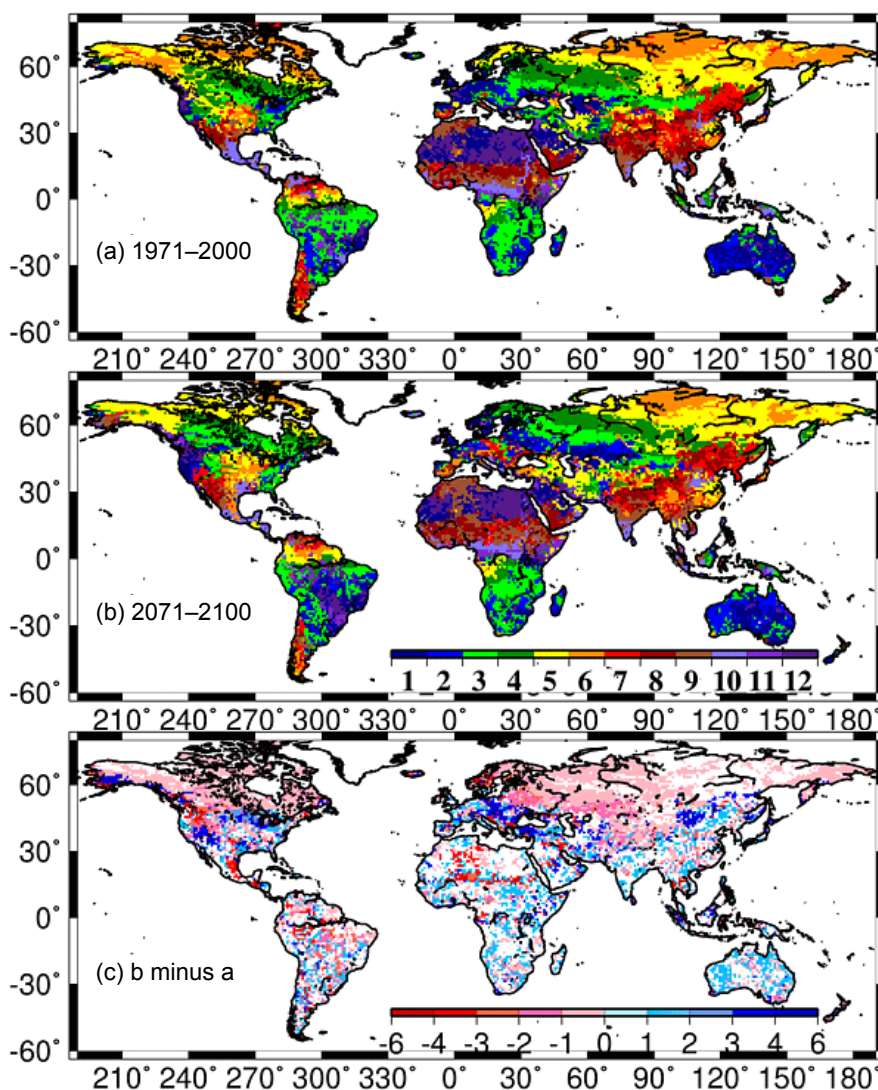


Fig. 7 Month of annual maximum daily discharge during: (a) 1901–2000, (b) 2071–2100 and (c) the difference between them estimated by the MIROC.

peak discharge likely reflects a change in the flood season from springtime snowmelt to summer-time heavy precipitation. The shift in flood season and the change in the type of flood may require changes in river management within these regions to protect against flood disasters in unexpected seasons.

4 DROUGHT

Drought events were defined by the number of days when daily discharge was lower than the tenth percentile of all river discharge data from the 20th century simulation (Q_{90}). The Q_{90} was estimated for each calendar day (1–365) using the variable threshold level method (Hisdal *et al.*, 2001). The minimum thresholds for drought conditions were determined by ranking discharge data from largest to smallest for each individual day of the year. The 21-day samples from a moving window before and after the calendar day were used to increase the number of samples. For example, 21 days, from 1 January to 21 January, were used to obtain the Q_{90} on 11 January for 1901–2000 (a total of 2100 samples).

Before estimating drought in the GRDC, a simple statistical test for annual mean discharge for the GRDC data was used, because observed low flow can be affected by artificial discharge controls such as large reservoirs. The time series of annual average gauge observations were divided into two, and the two samples were tested using a one-sample Student's *t* test to detect statistical jumps in the time-series. This method can be used to detect the construction of large dams, such as the Grand Coulee Dam in 1942 on the Colorado River. Jumps in annual discharge occurred at 352 stations from the 724 GRDC gauges. This method detected no statistical jumps over regions including Europe, eastern Canada, or Australia. Three possible reasons could explain the lack of jumps in these areas. First, most large dams were constructed before the first year of available data. Second, gauge data in these countries were processed using a gap-filling method. Third, the range of annual discharge has large natural variation. The first and the second reasons may explain the lack of a statistical jump for Europe, whereas the third reason may account for the lack of a statistical jump in Australia. Stations with data jumps were not used in the estimation of drought.

4.1 Drought validation

As in the case of flood validation, annual drought days in the MIROC that were used to define drought were also checked with the observations and off-line simulation. The number of annual drought days in the off-line simulation was first validated against the number of observations by examining the correlation coefficients (Fig. 8). The observed annual drought days were adequately reproduced globally by the off-line simulation, suggesting that the land surface sub-module of the MIROC has the potential to estimate drought frequency in the discharge record. As explained above, the MIROC is a coupled ocean–atmosphere–land model and its climate may be statistically similar to observed patterns, but not necessarily similar at daily time intervals. Consequently, the characteristics of drought days, rather than year-to-year correlation coefficients should be evaluated. However, it is difficult to validate the characteristics of drought days estimated by the MIROC because drought is defined by the relative Q_{90} from long-term data. Therefore, this study assumed that the MIROC model with the MATSIRO land surface sub-module estimated the relative change in projected future drought conditions, because relative changes in the Q_{90} between the 20th century and future simulations in the MIROC can be projected.

As in the case of flood, a drought day was evaluated whether it reflected historical disastrous drought or not. Estimated annual drought days in the off-line simulation were compared with those from the gauge observations for times for which disastrous droughts were recorded in the EM-DAT disaster database. Because this study did not use the observed discharge data that had artificial discharge controls for the drought validation, data availability was less than that for the flood validation, especially for developed countries. In contrast, available data from developing

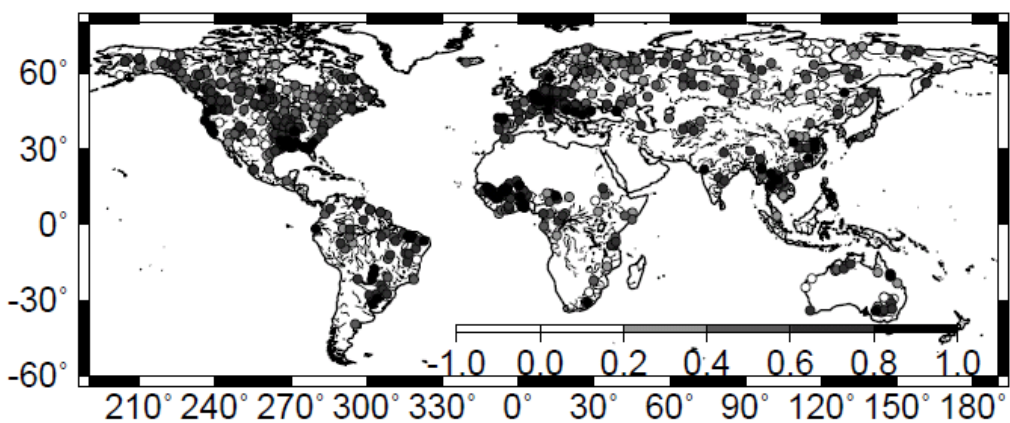


Fig. 8 Correlation coefficient of the number of annual drought days between gauge observation and off-line simulation.

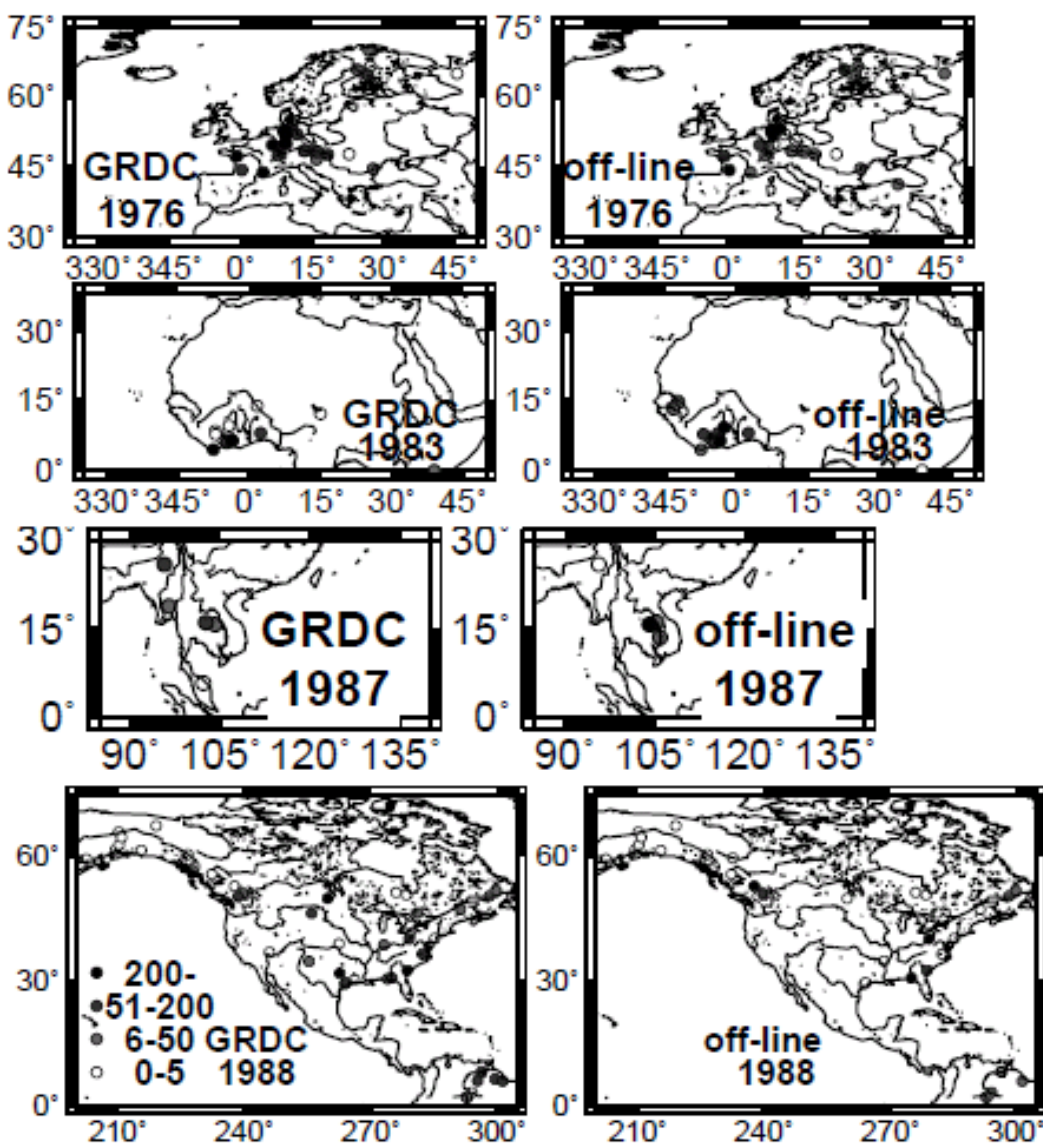


Fig. 9 Number of the annual drought days estimated from gauge observation (left) and off-line simulation (right).

countries are very limited for the off-line simulation because of the poor quality of precipitation input. As a result, the number of stations available for the drought validation was much more limited than for the flood validation, and the number of available stations sometimes differed between the off-line simulation and the observations. Figure 9 shows examples of drought estimates when severe droughts were recorded in the EM-DAT. Because drought is a spatially distributed disaster and detailed information with which to specify the location (e.g. the river name) is not implemented in the EM-DAT database, the geographic distribution of drought days rather than a comparison of specific rivers was examined. In 1976, both the observations and off-line simulations show more than 50 drought days in Europe. Drought spells longer than 50 days also occurred in the regions of the Sahel in 1983, along the Mekong River in 1987, and on the northwestern coasts and the southeastern North America in 1988. Annual drought spells longer than several tens of days seem to have some relation to the occurrence of disastrous drought.

4.2 Projecting future drought

The statistical significance of changes in annual drought days was determined using a Monte Carlo approach (Fig. 10). Similar to the analysis for projecting change in future flood, 1000 multiple Monte Carlo simulations were conducted using 30 random samples of annual drought days from the 20th century (1901–2000) simulation. The averages of the 1000 sets of the 30 samples were compared with the average of annual drought days in the future climates (2001–2030 and 2071–2100). Annual drought days were calculated based on Q_{90} discharge defined by daily discharge data for 1901–2000 in every case.

Changes in drought are indicated by the ratio of annual drought days, e.g. the averaged annual drought days in the future divided by the averaged annual drought days in the 20th century simulation (Fig. 11). Regions that had no significant change in annual drought days (Fig. 10) were screened out. A significant increase in drought frequency is projected as an increase in the number

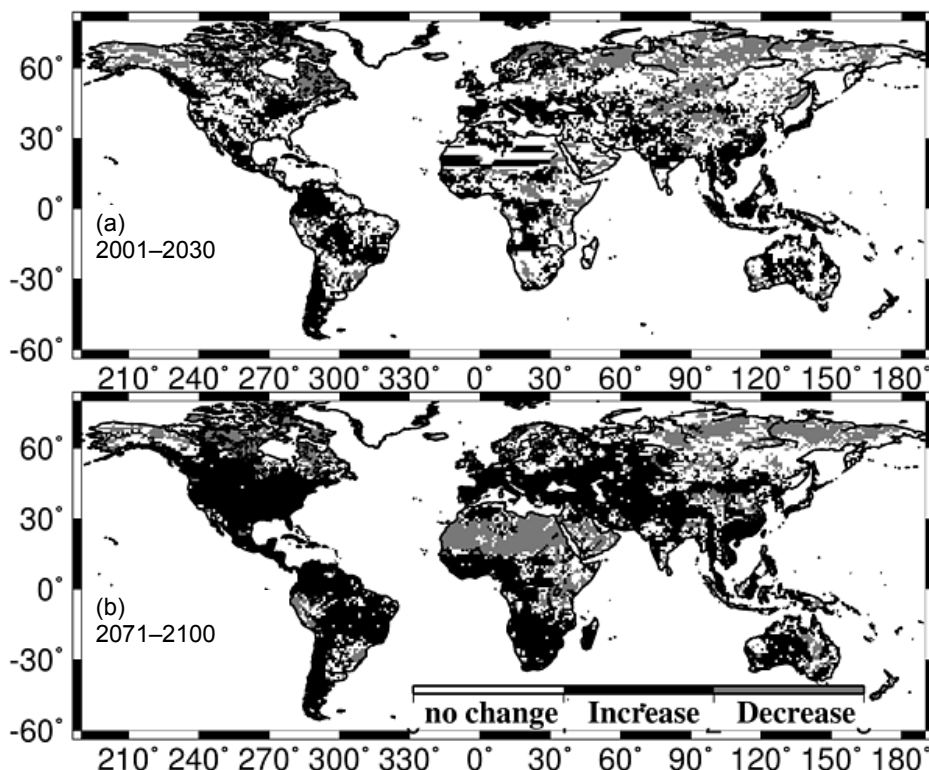


Fig. 10 Statistical significance of changes in annual drought days of: (a) the first and (b) the last 30 years of the 21st century against those in the 20th century (1901–2000) estimated by MIROC.

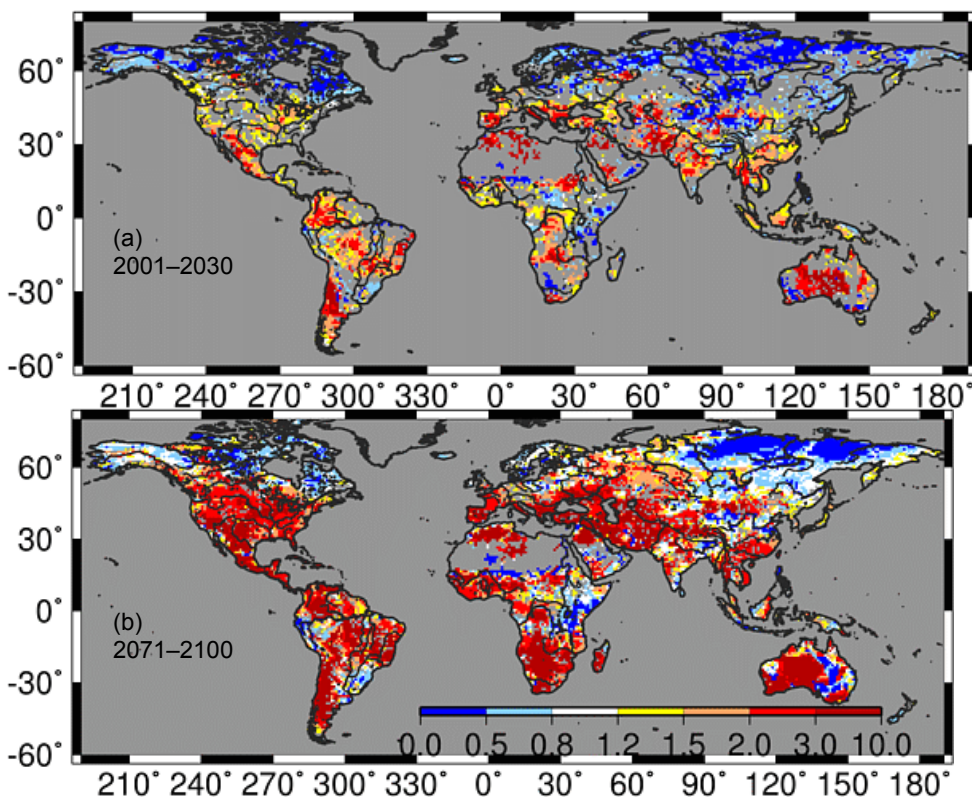


Fig. 11 Ratio of average number of annual drought days of: (a) 2001–2030 and (b) 2071–2100 to present-day (1901–2000) simulation.

of drought days during the last 30 years of the 21st century over North and South America, central and southern Africa, the Middle East, southern Asia from Indochina to southern China, and central and western Australia. Some regions, including Eastern Europe to central Eurasia, inland China, and northern North America, show increases in drought, but also show increases in annual precipitation (Fig. 1). In contrast, wide areas over eastern Russia show a decrease in drought days. These areas are the regions that have large increases in annual precipitation and marked increases in flood flows (e.g. Figs 1 and 6).

5 REASONS FOR CHANGES IN EXTREMES IN LARGE RIVER BASINS

Global analyses of flood and drought have suggested that the investigation of relationships between changes in flood and drought frequencies and changes in climate forcing are complex. In this section, a detailed analysis for global large river basins is described to illustrate possible relationships between changes in flood and drought and changes in other hydrological components.

Table 2 summarizes future changes predicted by MIROC simulations, over 30 large river basins, as defined by the $1^\circ \times 1^\circ$ TRIP model, shown in Fig. 12. Changes in flood, drought and annual discharge were estimated at the basin outlets; other values were averaged over whole basins. Rivers in Fig. 12 were classified as high-latitude (nos 1–6), mid-latitude (7–20) and low-latitude (21–30) rivers. The shaded cells in Table 2 indicate increases in flood frequency (expressed as a decrease in the return period defined for a 20C 100-year flood from 1901–2000) and increases in drought frequency (i.e. the ratio of averaged drought days in 2071–2000 to that in 1901–2000 is >1.0). Negative differences in other components between the 21st century and 20th century are also shaded. The value of the PPCC for 1971–2000 is also shown in Table 2. All except two basins had PPCC values higher than 0.95. We also determined the time period at which

Table 2 Future changes projected by MIROC simulation, over 30 large river basins.

	PPCC for 1971–2000	Return period of 20C 100- year flood ^(a) (year)	Ratio of drought days ^(b) (-)	Diff. in annual P ^(c) (mm/d)	Diff. in evapotrans- piration ^(c) (mm/d)	Diff. in annual fourth largest P ^(c) (mm/d)	Diff. in rain days ^(c) (d)	Diff. in $P - E$ ^(c) (mm/d)	Diff. in annual Q ^(c) (%)	Diff. in peak month of Q ^(c) (month)	Diff. in T ^(c) (K)	Period of flood change	Period of drought change	
1	Yukon	0.98	351.9	1.44	0.66	0.24	5.22	22.89	0.41	25.7	0.01	6.76	2060	—
2	Mackenzie	0.98	341.0	2.72	0.41	0.27	3.62	16.21	0.14	16.3	-0.96	6.66	2060	2075
3	Ob	0.97	162.3	1.91	0.29	0.23	3.04	11.78	0.06	16.6	-1.10	6.81	2045	—
4	Yenisey	0.97	32.7	0.20	0.41	0.22	4.06	18.89	0.19	39.0	-0.63	6.58	2015	—
5	Lena	0.98	5.6	0.02	0.35	0.14	4.51	13.26	0.22	40.5	-0.41	6.18	2015	2075
6	Kolyma	0.97	6.4	0.22	0.52	0.14	5.09	21.35	0.38	36.0	-1.00	6.34	2015	—
7	Rhein	0.97	328.7	1.89	0.14	0.23	4.03	-5.97	-0.09	-6.9	0.35	4.38	2085	2075
8	Donau	0.98	292.2	2.92	0.08	0.20	3.78	-7.91	-0.12	-6.5	2.50	4.84	2045	2015
9	Dniepr	0.98	2453.5	3.37	0.19	0.31	3.15	2.04	-0.12	-31.2	-0.55	5.16	2045	2015
10	Volga	0.96	671.0	3.40	0.21	0.31	2.84	4.65	-0.09	-14.9	-1.13	6.34	2045	2030
11	Amur	0.98	19.9	0.63	0.36	0.21	6.03	5.14	0.15	29.3	0.59	5.81	2030	—
12	Columbia	0.97	3.0	3.40	0.36	0.34	5.11	-4.31	0.02	-1.0	-2.72	5.35	2015	2015
13	Nelson	0.98	1.33×10^5	3.34	0.14	0.21	1.90	5.28	-0.06	-17.8	-0.89	6.57	2045	2030
14	St Lawrence	0.98	463.1	2.60	0.16	0.34	4.89	-5.58	-0.18	-15.2	0.68	6.14	2045	2030
15	Mississippi	0.97	149.6	3.93	-0.16	0.00	2.21	-9.42	-0.16	-22.0	0.27	6.14	2060	2060
16	Colorado	0.96	1.82×10^9	4.19	-0.17	0.00	0.32	-11.04	-0.17	-42.9	1.42	6.43	2045	2030
17	Yellow	0.97	2.3	0.00	0.65	0.39	7.67	13.62	0.26	46.7	0.14	5.13	2015	2045
18	Yangtze	0.97	44.6	0.69	0.45	0.23	8.04	0.33	0.22	15.0	-0.57	5.05	2030	—
19	Murray	0.94	19.0	0.80	-0.01	-0.07	3.11	-7.79	0.06	83.0	0.44	4.35	2015	—
20	Zambezi	0.97	223.7	3.94	-0.19	-0.01	3.87	-13.48	-0.18	-21.4	0.45	5.07	2045	2060
21	Niger	0.95	11.9	2.59	0.22	0.12	11.56	-6.90	0.10	7.6	-1.40	5.10	2030	2015
22	Congo	0.97	89.7	2.80	0.03	0.27	10.84	-21.99	-0.24	-1.3	0.24	4.51	2075	—
23	Nile	0.95	15.7	0.07	0.25	0.04	7.44	-6.15	0.21	19.7	0.08	4.55	2030	—
24	Euphrates	0.93	3647.2	4.00	-0.22	-0.15	-0.58	-12.63	-0.07	-53.8	0.10	5.15	2045	2030
25	Indus	0.96	104.9	4.05	0.09	0.12	1.99	-2.87	-0.02	-12.5	0.28	6.02	2060	2015
26	Ganges	0.97	26.1	1.17	0.23	-0.02	10.64	-8.19	0.25	17.6	0.40	5.07	2060	—
27	Brahmaputra	0.97	3.8	0.15	1.91	0.30	26.53	6.41	1.61	32.4	-0.30	5.81	2015	2045
28	Mekong	0.97	104.7	1.20	0.29	0.17	10.94	-14.23	0.12	10.6	-1.17	4.48	—	—
29	Orinoco	0.97	5367.0	3.82	-0.79	-0.01	5.92	-30.80	-0.79	-29.4	-0.99	5.18	2045	2015
30	Amazon	0.98	238.2	3.31	-0.18	-0.10	10.64	-22.80	-0.08	-1.9	-0.99	5.44	2085	2030

(a) Future (2071–2100) return period of 20th century 100-year discharge defined by annual maximum discharge during 1901–2000.

(b) Ratio between drought days of 2071–2100 and drought days of 1901–2000.

(c) Difference between values in 2071–2100 and 1901–2000 of: annual precipitation (P), annual evapotranspiration, annual fourth largest precipitation, number of annual rain days, annual precipitation minus annual evapotranspiration, annual river discharge (Q), month of annual maximum daily discharge, and annual mean surface temperature.

The last two columns indicate time period when the projecting future changes in flood and drought are first detected.

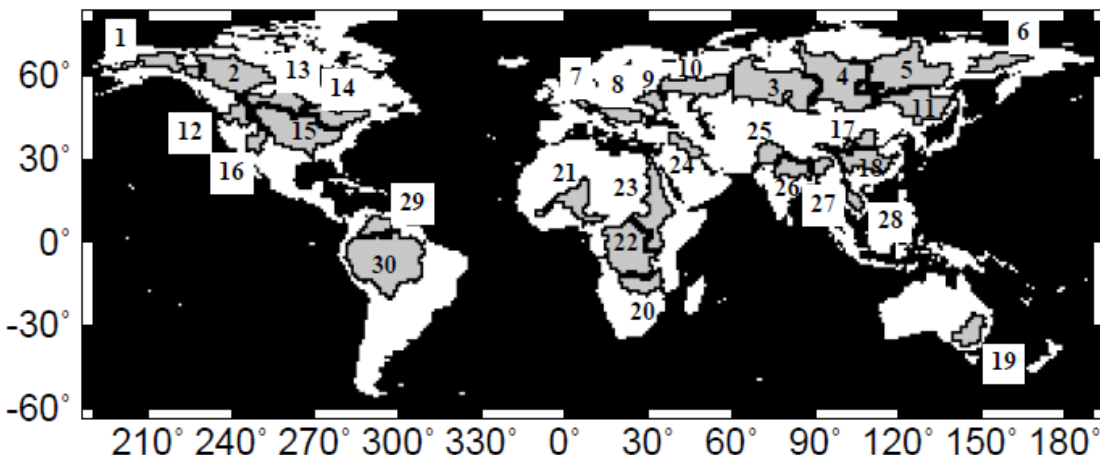


Fig. 12 Selected 30 river basins.

the projected future changes in floods and droughts are first visible by indicating middle years of 30-year samples (e.g. 2015 indicates the period from 2001 to 2030) when the changes compared to the values from 1901 to 2000 first become statistically significant.

Many basins experience an increase in heavy precipitation (the fourth heaviest annual daily precipitation) and temperature in the future scenario (Table 2). High-latitude river basins also experience increase in annual precipitation, evapotranspiration, precipitation minus evapotranspiration ($P - E$), and number of precipitation days in the future. Precipitation days are projected to decrease over low-latitude river basins, except for the Brahmaputra River.

The relationship between annual discharge and frequency of 20C 100-year flood varies; 11 of the 13 rivers that show an increase in frequency of 20C 100-year flood also show an increase in annual discharge; the exceptions are the Columbia and Congo rivers (Table 2). Because return period of a 20C 100-year flood on the Columbia River varied widely among basin grid points (not shown), the return period estimated at the basin outlet in the Table 2 does not represent the return period of the basin. Thus, the Columbia River is considered an exception. The Congo River is also treated as an exception because the change in the return period is relatively small (89.7 years), as is the projected change in annual discharge (-1.3%). Rivers with an increase in frequencies of 20C 100-year flood also exhibit an increase in annual discharge, but rivers that show an increase in annual discharge do not necessarily show an increase in frequencies of 20C 100-year flood. Four rivers (i.e. the Yukon, Mackenzie, Ob and Mekong) are predicted to have a decrease in frequencies of 20C 100-year flood, even though the annual discharge is estimated to increase. Decreases in the frequencies of 20C 100-year flood on the Yukon, Mackenzie and Ob rivers may result from earlier and smaller maximum discharge at northern high latitudes because of decreased snow accumulation under the warming climate. In summary, river basins at mid- to low-latitudes in which frequencies of 20C 100-year flood increase also show an increase in the annual discharge; however, an increase in annual discharge does not always a signal of an increase in floods at some high-latitude rivers, where the annual maximum daily discharge occurs during snowmelt.

There was a relationship between changes in drought frequency and changes in $P - E$. Changes in annual precipitation had a smaller effect than changes in $P - E$ on changes in drought. The Rhein, Donau, Dniepr, and Volga rivers in Europe; the Nelson and St Lawrence rivers in northern North America; the Congo River; and the Indus River were all projected to have increases in drought frequency, despite increases in annual precipitation. The increase in evapotranspiration during 2071–2100 in these basins is much higher than the increase in precipitation (see Fig. 1), perhaps because of the increase in surface temperature of 4 to 6°C during the same period. Changes in drought over a river basin should therefore be predicted based on changes in $P - E$, rather than changes in the annual amount of precipitation only.

River basins characterized by decreases in $P - E$ in the 21st century show increases in drought, but an increase in drought does not necessarily result in a decrease in $P - E$ (Table 2). Drought increased in six basins (i.e. the Yukon, Mackenzie, Ob, Columbia, Niger and Ganges basins) when the values of both $P - E$ and annual discharge were projected to increase in the 21st century. Three of the six rivers are located at high-latitude (i.e. the Yukon, Mackenzie, and Ob rivers) and have only small increases in the proportion of drought days. As is the case of flood, because the estimated drought frequency on the Columbia River varied widely among the basin grids (not shown), and the changes in $P - E$ between the 21st and 20th centuries are small (+0.02 mm/d), the Columbia River was again treated as an exception. The other two rivers (i.e. the Niger and Ganges) show increases in both flood and drought, as also does the Congo River. These three river basins have a large increase in heavy precipitation (more than 10 mm/d) and a large decrease in precipitation days (10 days or more). Such a change in the precipitation pattern may cause an increase in drought days even though precipitation, discharge, and $P - E$ increase.

In addition, an increase or decrease in flood frequency appeared before the middle of the 21st century in 21 of the 30 basins (Table 2). In contrast, 14 basins showed a significant change in drought frequency in the first half of the 21st century; 12 of these 14 basins showed a significant increase in drought days. This suggests that significant future increases in drought appear relatively early under the projected climate, compared to significant decreases in drought.

6 CONCLUSIONS

Climate change is expected to accelerate global hydrological cycles. River discharge will increase on a global scale because of the increased precipitation and reduced evapotranspiration. Studies of extremes in hydrology at short time scales are considered indispensable (Oki & Kanae, 2006). Previous studies have typically focused on averages of river discharge, and few studies show global projections of extremes in river discharge. This paper considered the frequencies of future floods and droughts as estimated by a relatively high-spatial-resolution coupled ocean–atmosphere–land GCM (MIROC) and presents the global validation of extreme discharge in the MIROC using 724 long-term daily gauge observations and a long-term off-line simulation by the land surface sub-model (MATSIRO). The results indicate that the MIROC has the potential to reproduce historical disastrous floods and droughts. Discharges that have a return period longer than 30 years, and annual drought days of more than 50 days, were found to be related to several past historical disasters, even though their values were roughly extracted from limited case studies and further study is needed.

Floods and droughts projected for the 21st century show significant and large changes from those in the 20th century (i.e. from 1901 to 2000). The results indicate an increase in the frequency of floods in many regions of the globe, except regions including North America and central and western Eurasia. Increases in the number of drought days during the last 30 years of the 21st century are significant over regions such as North and South America, central and southern Africa, the Middle East, central to western Australia, and Indochina to southern China.

Analyses over large river basins reveal the complexity of possible changes in future floods and droughts. Changes in floods and droughts cannot be explained by changes in annual precipitation, annual evapotranspiration, or the difference between annual precipitation and annual evapotranspiration. Although rivers with an increase in floods also exhibit increase in annual discharge, rivers with an increase in the annual discharge do not necessarily show an increase in floods in regions where the annual maximum discharge occurs during snowmelt. In contrast, river basins characterized by decreases in $P - E$ in the 21st century show increases in drought, but an increase in drought does not necessarily result in a decrease in $P - E$. The changes in precipitation patterns may cause an increase in the number of drought days even though precipitation, discharge, and $P - E$ increase. The comparison of flood and drought frequencies estimated from daily discharge is therefore important in predicting future discharge extremes. Several regions showed changes in the flood season. Many regions in the northern high latitudes show an earlier flood season mainly

because of earlier snowmelt under the warming climate. Some regions show changes in the flood season from the snowmelt season to the summer because of heavy precipitation.

The GCM in this paper is the only model with relatively higher spatial resolution at present, which is comparable with daily discharge of gauge observation and global off-line simulations. Given the non-linear uncertainty of GCMs, multi-model ensemble projections and analyses should be indispensable. Because the IPCC data distribution centre (<http://www.ipcc-data.org/>) do not provide daily discharge data, one possible way to estimate multi-model GCM projections in extreme river discharge is to run a land surface model using atmospheric forcing by the multi-GCMs. However, because of the current limitation of other GCMs in terms of spatial resolution, direct use of discharge data by those models is not applicable to resolve extremes of daily river discharge, since the difference in meteorological features between higher (T106, approximately 1.1 degree) and middle (T42, 2.8-degree) GCMs is large (Kimoto *et al.*, 2005). Moreover, the method using off-line simulation loses land-atmosphere feedback information. It is also concerning that the inconsistency of land surface condition between a land surface model used for the off-line simulation and land surface sub-modules of GCMs may affect the result. Future global warming experiments by other GCMs with higher spatial resolution are therefore expected in the future to obtain multi-model projection of daily discharge extremes.

The projected increases of frequencies in flood and drought in many regions globally indicate that the global water cycle in MIROC is intensified due to radiative effects of anthropogenic changes in atmospheric composition. Future increases or decreases in flood frequency were apparent before the middle of the 21st century in 21 of the 30 basins selected. Twelve of these basins showed a significant increase in drought frequency in the early 21st century. The results indicate that we have a potential to detect or attribute the changes in discharge extremes in the near future, or the change may be already occurring and detectable from historical discharge, as was done for average precipitation by Zhang *et al.* (2007). However, trend analysis of the maximum daily discharge is only available at four stations, because the number of available long-term daily observations of river discharge is much smaller than that of precipitation, and because the artificial water usage severely effects long-term variation of the observed discharge. The intensification in discharge extremes is therefore not easily detectable from observations or current GCMs without considering anthropogenic water usage. Future development of GCMs to include human control on discharge and intensive long-term daily discharge observations will help in further analyses.

Acknowledgements We thank the GRDC for providing daily discharge observations. This research was supported by the JSPS Postdoctoral Fellowships for Research Abroad, the Global Environment Research Fund of the Ministry of Environment (B-12 and S-5) and the innovation program of climate change projection for 21st century of the Ministry of Education, Culture, Sports, Science, and Technology of Japan.

REFERENCES

- Andreadis, K. M., Clark, E. A., Wood, A. W., Hamlet, A. F. & Lettenmaier D. P. (2005) Twentieth-century drought in conterminous United States. *J. Hydromet.* **6**, 985–1001.
- Beven, K. J. & Kirkby, M. J. (1979) A physically based variable contributing area model of basin hydrology. *Hydrolog. Sci. Bull.* **24**, 43–69.
- Brakenridge, G. R., Anderson, E. & Caquard, S. (2003) Flood inundation map DFO 2003–282. Dartmouth Flood Observatory, Hanover, USA, digital media, <http://www.dartmouth.edu/flood/2003282.html>.
- Dai, A., Trenberth, K. E. & Qian, T. (2004) A global dataset of Palmer Drought Severity Index for 1870–2002. *J. Hydromet.* **5**, 1117–1130.
- Emori, S., Hasegawa, A., Suzuki, T. & Dairaku, K. (2005) Validation, parameterization dependence, and future projection of daily precipitation simulated with a high-resolution atmospheric GCM. *Geophys. Res. Lett.* **32**, doi:10.1029/2004GL022306.
- Famiglietti, J. S. & Wood, E. F. (1991) Evapotranspiration and runoff from large land areas: land surface hydrology for atmospheric general circulation models. *Surv. Geophys.* **12**, 179–204.
- Gumbel, E. J. (1941) The return period of flood flows. *Ann. Math Statist.* **12**, 163–190.
- Hirabayashi, Y., Kanae, S., Struthers, I. & Oki, T. (2005) A 100-year (1901–2000) global retrospective estimation of terrestrial water cycle. *J. Geophys. Res. Atm.* **110**, doi:10.1029/2004JD005492.

- Hisdal, H., Stahl, K., Tallaksen, L. M. & Demuth, S. (2001) Have streamflow droughts in Europe become more severe or frequent? *Int. J. Climatol.* **21**, 317–333.
- IPCC (Intergovernmental Panel on Climate Change) (2000) *Special Report on Emissions Scenarios* (ed. by N. Nakicenovic & S. Swart). Cambridge University Press, Cambridge, UK.
- Kanae, S., Oki, T. & Kashida, A. (2004) Changes in hourly heavy precipitation at Tokyo from 1890 to 1999. *J. Met. Soc. Japan* **82**(1), 241–247.
- Kanae, S., Hirabayashi, Y., Yamada, T. & Oki, T. (2006) Influence of “realistic” land-surface wetness on predictability of seasonal precipitation in boreal summer. *J. Climate* **19**, 1450–1460.
- Kimoto, M., Yasutomi, N., Yokoyama, C. & Emori, S. (2005) Projected changes in precipitation characteristics near Japan under the global warming. *SOLA* **1**, 85–88, doi:10.2151/sola.2005-023.
- Kunkel, K. E., Easterling, D. R., Redmond, K. & Hubbard, K. (2003) Temporal variations of extreme precipitation events in the United States: 1895–2000. *J. Geophys. Res.* **30**, CLM5-1-5-4.
- K-1 model developers (2004) K-1 coupled model (MIROC) description. Technical report, Center for Climate System Research, University of Tokyo, Tokyo, Japan.
- Milly, P. C. D., Wetherald, R. T., Dunne, K. A. & Delworth, T. L. (2002) Increasing risk of great floods in a changing climate. *Nature* **415**, 514–517.
- Milly, P. C. D., Dunne, K. A. & Vecchia, A. V. (2005) Global pattern of trends in streamflow and water availability in a changing climate. *Nature* **438**, 347–350, doi:10.1038/nature04312.
- Mitchell, T. D. & Jones, P. (2005) An improved method of construction a database of monthly climate observations and associated high-resolution grids. *Int. J. Climatol.* **25**, 693–712.
- Nijssen, B., Schnur, R. & Lettenmaier, D. P. (2001a) Global retrospective estimation of soil moisture using the Variable Infiltration Capacity land surface model, 1980–93. *J. Climate* **14**, 1790–1808.
- Oki, T. & Sud, Y. C. (1998) Design of Total Runoff Integrating Pathways (TRIP)—A global river channel network. *Earth Interactions* **2**, 1–37.
- Oki, T. & Kanae, S. (2006) Global hydrologic cycles and world water resources. *Science* **313**, 1068–1072, doi:10.1126/science.1128845.
- Oki, T., Nishimura, T. & Dirmeyer, P. (1999) Assessment of annual runoff from land surface models using Total Runoff Integrating Pathways (TRIP). *J. Met. Soc. Japan* **77**, 235–255.
- Palmer, W. C. (1965) Meteorological drought. Tech. report, US Dept. of Commerce, USA.
- Sellers, P. J., Randall, D. A., Collatz, G. J., Berry, J. A., Field, C. B., Dazlich, D. A., Zhang, C., Collelo, G. D. & Bounoua, L. (1996) A revised land surface parameterization (SiB2) for atmospheric GCMs. Part I: Model formulation. *J. Climate* **9**, 676–705.
- Stieglitz, M., Rind, J., Famiglietti, J. & Rosenzweig, C. (1997) An efficient approach to modeling the topographic control of surface hydrology for regional and global climate modeling. *J. Climate* **10**, 118–137.
- Takata, K., Emori, S. & Watanabe, T. (2003) Development of the minimal advanced treatments of surface interaction and runoff. *Global Planet. Change* **38**, 209–222.
- Vogel, R. M. (1986) The probability plot correlation coefficient test for the normal, lognormal, and Gumbel distributional hypotheses. *Water Resour. Res.* **22**, 587–590.
- Watanabe, T. (1994) Bulk parameterization for a vegetated surface and its application to a simulation of nocturnal drainage flow. *Boundary-Layer Met.* **70**, 13–35.
- Yokohata, T., Emori, S., Nozawa, T., Ogura, T., Okada, N., Suzuki, T., Tsushima, Y., Kawamiya, M., Abe-Ouchi, A., Hasumi, H., Sumi, A. & Kimoto, M. (2007) Different transient climate responses of two versions of an atmosphere-ocean coupled general circulation model. *Geophys. Res. Lett.* **34**, L02707, doi:10.1029/2006GL027966.
- Zhang, X., Zwiers, F. W., Hegerl, G. C., Lambert, F. H., Gillett, N. P., Solomon, S., Stott, P. A. & Nozawa, T. (2007) Detection of human influence on twentieth-century precipitation trends. *Nature* **448**, 461–465.

Received 1 June 2007; accepted 28 April 2008